2018 European Control Conference (ECC)
June 12-15, 2018. Limassol, Cyprus

Multiple Model Adaptive ILC for Human Movement Assistance

C. T. Freeman[1], K. L. Meadmore[2], A.-M Hughes[2], N. Grabham[1], J. Tudor[1], K. Yang[1]

***Abstract*— A switched multiple model iterative learning control framework is developed which guarantees robust stability and performance bounds under the assumption that the true plant belongs to a plant uncertainty set that is specified by the designer. In addition, the framework automatically adapts the reference trajectory according to the action of an existing internal control loop that is assumed to be embedded in the plant structure. The framework is inspired by the needs of stroke rehabilitation where assistive technology must support the remaining, weak volitional effort of the patient. Exploiting the multiple model based switching between models and reference trajectories, the framework is also able to potentially eliminate the need for identification and tuning and hence meet the demanding needs of clinical application.**

I. INTRODUCTION

Iterative learning control (ILC) is an approach formulated for systems that track the same output trajectory over multiple attempts, termed trials. Numerous algorithms have been proposed that update the control input in the reset interval between trials, with the aim of sequentially reducing the tracking error. A rich theoretical framework has emerged, together with a wide range of application fields. In particular, ILC has been successfully used by many groups to assist lower limb motion [19], [16], [2], [1]. ILC was first applied to upper limb stroke rehabilitation in [11], where it controlled the functional electrical stimulation (FES) applied to artificially activate patients' muscles. The movement accuracy produced by ILC led to statistically significant results in a clinical trial. ILC has since been used in further clinical trials to assist more complex movements involving the arm, wrist and hand [11], [15], [14], again producing statistically significant improvements in function.

While ILC can accurately assist completion of a predefined motion trajectory, the framework has not been able to respond to the voluntary effort contribution of each stroke participant. Not only does this cause the tracking accuracy to degrade, but any mismatch between voluntary intention and assisted movement also reduces the rehabilitation effectiveness [6]. Clinical application also restricts the time available for model identification and controller tuning, necessitating greater robust performance over a wide uncertainty space.

This paper addresses both issues by developing the first ILC framework to automatically adapt the reference trajectory in response to the residual capability of user, while simultaneously ensuring convergence to the intended task. This means that it can achieve high accuracy tracking of the motion that the participant is themselves attempting and thereby maximizes clinical outcomes. The framework is built on the estimation based multiple model switched adaptive control developed in [3], [4] and further extended for ILC in [8] to become estimation based multiple model ILC (EMMILC). These use a bank of Kalman filters to assess the performance of a set of candidate plant models, and the controller corresponding to the most suitable plant model is then switched into closed-loop. Given sufficient candidate models, the framework is able to guarantee robust performance. This feature is highly attractive within stroke rehabilitation since it theoretically removes the need for time-consuming model identification and control tuning.

[1]Electronics and Computer Science, University of Southampton, UK. Corresponding author Chris Freeman, cf@ecs.soton.ac.uk.
[2]Faculty of Health Sciences, University of Southampton, UK.

II. PROBLEM FORMULATION

Many models have been proposed for human motor control, usually splitting the action of the central nervous system (CNS) into path planning and subsequent tracking stages. Approaches can be divided into those that attempt to simulate the internal feedback/feedforward mechanisms present in the CNS, and those that try only to model the resulting kinematic motion at the task level. The latter typically pose reaching tasks as optimization problems, involving, e.g., the minimization of jerk [5], torque change [20], variance [10], interaction torques or a combination [17]. These forms can be represented by first defining a motion 'kernel' $\tilde{r}$ that captures the essential features of the known task. This comprises a sequence of p desired joint positions/velocities that must occur at isolated, potentially unknown, time points or intervals in a finite duration. Hence $\tilde{r} \in \mathbb{R}^{o_1} \times \cdots \times \mathbb{R}^{o_p}$. This is translated to an ideal movement of o joints specified over a sufficiently long sampling interval $[0, T]$, $T \in \mathbb{N}$, by operator $\tilde{B} : \mathbb{R}^{o_1} \times \cdots \times \mathbb{R}^{o_p} \mapsto l_2^o[0, T]$. CNS feedforward and feedback action can be modelled by operators $\tilde{K}_{\text{fb}} : l_2^o[0, T] \mapsto l_2^m[0, T]$, $\tilde{K}_{\text{ff}} : l_2^o[0, T] \mapsto l_2^m[0, T]$ respectively which produce electrical nerve signal $\tilde{v}$ that is transmitted to the musculoskeletal system represented by operator $\tilde{F} : l_2^m[0, T] \to l_2^o[0, T]$. In this paper FES is assumed to be

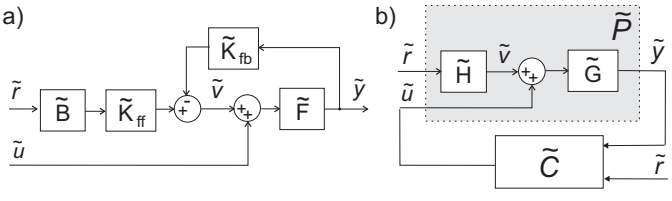

Fig. 1. a) 'along the trial' model of stimulated arm with volitional effort and applied assistance, b) equivalent system with controller $\tilde{C}$.

the rehabilitative technology employed, however mechanical support may alternatively be used. Accordingly, applied

FES to assist the m muscles involved in the movement is represented by additive signal $\tilde{u}$, as shown in Fig. 1a). These combine in a static manner [13] which may be assumed to be linear [12]. These forms can be expressed as the general structure of Fig. 1b) by setting $\tilde{H} = \tilde{K}_{\rm ff}\tilde{D}$, $\tilde{G} = (I + \tilde{F}\tilde{K}_{\rm fb})^{-1}\tilde{F}$. It follows that $\tilde{G}$ can be expressed by the causal linear time-invariant (LTI) state-space system (A_G, B_G, C_G) and $\tilde{H}$ is a non-casual along the trial mapping.

Due to stroke impairment, $\tilde{K}_{\rm fb}$, $\tilde{K}_{\rm ff}$ are difficult to identify. It must therefore be assumed that system $\tilde{P} : \tilde{y} = \tilde{G}(\tilde{H}\tilde{r} + \tilde{u})$ is unknown but belongs to a specified uncertainty set $\tilde{U}$. The objective is to control $\tilde{u}$ such that the closed-loop system is stable, and the output matches the intention of the CNS, i.e. the output achieves $\tilde{y} = \tilde{B}\tilde{r}$, where $\tilde{B}\tilde{r}$ is the reference trajectory. Since motion kernel $\tilde{r}$ contains the positions/velocities that capture the task, it is assumed to be known. In general $\tilde{B}$ is not known, however a set of feasible $\tilde{B}$ operators can be reliably generated, e.g. by applying the minimum jerk computation of [5] to a suitable set of times at which each joint position/velocity is reasonably achieved. For simplicity it is assumed that $o = m$ and $\tilde{G}$ is invertible.

A. Equivalent System Representation

We now reformulate the system in order to apply the EMMILC framework of [8]. First denote $\tilde{u}_{1,1} = \tilde{u}$, $\tilde{y}_{1,1} = \tilde{y}$ and replace $\tilde{r}$ by $\tilde{u}_{1,2}$. Then augment the plant and controller with additional outputs, $\tilde{y}_{1,2}$, $\tilde{u}_{2,2}$ respectively, and introduce external disturbances on all signals. Due to the repeated nature of the task, we can then express all signals as single samples in a 'lifted' space by defining repetition index superscript $k \in \mathbb{N}_+$ and $u_{i,j}(k) = \tilde{u}^k_{i,j}$, $y_{i,j}(k) = \tilde{y}^k_{i,j}$, $r(k) = \tilde{r}$. The corresponding operators

$$\begin{aligned} G &: l_2^m[0,T] \times \mathbb{N} \mapsto l_2^o[0,T] \times \mathbb{N} \\ &: w \mapsto y_{1,1} : y_{1,1}(k) = \tilde{G}w(k) \qquad (1) \\ H &: \mathbb{R}^{o_1} \times \cdots \times \mathbb{R}^{o_p} \times \mathbb{N} \mapsto l_2^m[0,T] \times \mathbb{N} \\ &: u_{1,2} \mapsto v : v(k) = \tilde{H}u_{1,2}(k) \qquad (2) \end{aligned}$$

are the lifted representations of along-the-trial dynamics $\tilde{G}$ and $\tilde{H}$. These definitions mean system Fig. 1b) can be equivalently represented as in Fig. 2, where $\bar{u}_0 = (0, r)^\top \in \mathcal{U}_e$, $\bar{y}_0 = (0, r)^\top \in \mathcal{Y}_e$, $u_i = (u_{i,1}, u_{i,2})^\top \in \mathcal{U}_e$, $y_i = (y_{i,1}, y_{i,2})^\top \in \mathcal{Y}_e$, $i \in \{0, 1, 2\}$ in which the lifted spaces

$$\begin{aligned} \mathcal{U} &:= l_2^m[0,T] \times \mathbb{R}^{o_1} \times \cdots \times \mathbb{R}^{o_p} \times \mathbb{N}, \\ \mathcal{Y} &:= l_2^o[0,T] \times \mathbb{R}^{o_1} \times \cdots \times \mathbb{R}^{o_p} \times \mathbb{N}, \qquad (3) \end{aligned}$$

with $w_i := (u_i, y_i)^\top \in \mathcal{U} \times \mathcal{Y}$, and lifted plant operator

$$P : \mathcal{U}_e \mapsto \mathcal{Y}_e : u_1 \mapsto y_1 : \begin{pmatrix} y_{1,1} \\ y_{1,2} \end{pmatrix} = \begin{pmatrix} G & GH \\ 0 & 0 \end{pmatrix} \begin{pmatrix} u_{1,1} \\ u_{1,2} \end{pmatrix} \in \mathcal{P} \qquad (4)$$

where $\mathcal{P}$ is the set of all LTI operators of appropriate dimension. The distance between system models will be measured using the well-established gap metric, $\delta(\tilde{P}, \tilde{P}_1)$, $\tilde{P}, \tilde{P}_1 \in \tilde{U}$, introduced in [9]. Note that it can be shown that unlifted and lifted gaps are equal, i.e. $\delta(\tilde{P}, \tilde{P}_1) = \delta(P, P_1)$ [7].

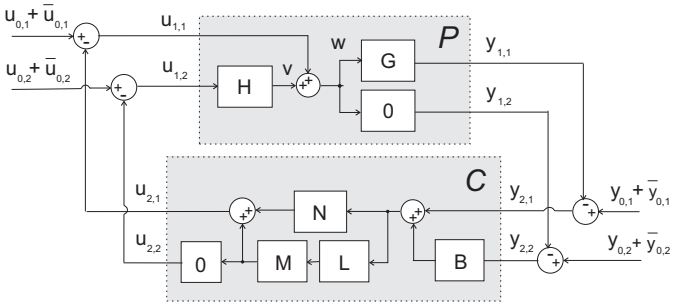

Fig. 2. Augmented lifted ILC system fitting within EMMILC framework.

III. CONTROLLER FORMULATION

In this section it is assumed that plant model $P = P_i$, with components H_i, G_i, is known. We must design controller $C_j \in \mathcal{C}$, with components N_j, L_j, B_j, to stabilise the system and satisfy tracking requirement $y_{1,1} = B_j r$. Here $\mathcal{C}$ is the set of all LTI operators of consistent dimension.

Proposition 1: Let $\tilde{H}_i$ be given and $\tilde{G}_i$ have state space form (A_G, B_G, C_G). The along-the-trial ILC objective

$$\min_{\substack{u_{1,1}(k) \in \\ l_2^m[0,T]}} \left\{ \|\tilde{B}_i\tilde{r} - y_{1,1}(k)\|^2_Q + \|u_{1,1}(k) - u_{1,1}(k-1)\|^2 \right\} \qquad (5)$$

is solved in the absence of disturbances by the control input

$$\begin{aligned} \tilde{u}_{2,1}(k,t) =& \tilde{u}_{2,1}(k-1,t) + \Phi(t)\big(\hat{x}(k,t) - \hat{x}(k-1,t)\big) \\ & - B_G^\top \xi(k,t) \qquad (6) \end{aligned}$$

with $\Phi(t) = (I + B_G^\top K(t) B_G)^{-1} B_G^\top K(t) A_G$, estimated state

$$\begin{aligned} \hat{x}(k,t+1) =& A_G\hat{x}(k,t) + B_G\big((\tilde{H}_i\tilde{r})(t) - \tilde{u}_{2,1}(k,t)\big) \\ & + O\big(C_G\hat{x}(k,t) + \tilde{y}_{2,1}(k,t)\big), \qquad (7) \end{aligned}$$

with observer matrix O, and the feedforward term

$$\begin{aligned} \xi(k,t) = \big(I + K(t)B_G B_G^\top\big)^{-1} \big\{ & A_G^\top \xi(k,t+1) + \\ & C_G^\top Q\big((\tilde{B}_i\tilde{r})(t+1) + \tilde{y}_{2,1}(k-1,t+1)\big)\big\} \qquad (8) \end{aligned}$$

with $\xi(k,T) = 0$ and $K(t)$ defined by

$$\begin{aligned} K(t) =& A_G^\top K(t+1)\big(I + B_G B_G^\top K(t+1)\big)^{-1} A_G + C_G^\top Q C_G, \\ & K(T) = 0 \qquad (9) \end{aligned}$$

Proof: Embeds $\tilde{H}_i$, $\tilde{B}_i$ within the structure of [18]. ■

To apply the multiple model switching framework it is necessary to express (6) - (9) in the lifted form as follows. Define the lifted integrator block which embeds ILC action

$$\begin{aligned} M &: l_2^m[0,T] \times \mathbb{N} \mapsto l_2^m[0,T] \times \mathbb{N} : z \mapsto x \\ &: x(k+1) = x(k) + z(k) \qquad (10) \end{aligned}$$

and $N_j : a \mapsto b : a(k) = \tilde{N}_j b(k)$, $B_j : a \mapsto b : a(k) = \tilde{B}_j b(k)$, $L_j : a \mapsto b : a(k) = \tilde{L}_j b(k)$.

Proposition 2: Control action (6) - (9) is realised by

$$\tilde{N}_j = \Xi_j, \tilde{B}_j = \tilde{B}_i, L_j = \big(\Xi_j\tilde{G}_i - I\big)\big(I + \tilde{G}_i^* Q \tilde{G}_i\big)^{-1}\tilde{G}_i^* Q \qquad (11)$$

where

$$\Xi_j = \begin{bmatrix} 0 & \cdots & \cdots & 0 \\ \Phi(1)O & 0 & \cdots & 0 \\ \vdots & \vdots & \ddots & \vdots \\ \Phi A_{\hat{x}}^{T-1}(T-1)O & \Phi A_{\hat{x}}^{T-2}(T-2)O & \cdots & 0 \end{bmatrix},$$

$$\tilde{G}_i = \begin{bmatrix} 0 & \cdots & \cdots & 0 \\ C_G B_G & 0 & \cdots & 0 \\ \vdots & \vdots & \ddots & \vdots \\ C_G A_G^{T-1} B_G & C_G A_G^{T-2} B_G & \cdots & 0 \end{bmatrix} \tag{12}$$

with $A_{\hat{x}}(t) = A_G - B_G\Phi(t) + OC_G = (I + B_G B_G^\top K(t))^{-1} A_G + OC_G$. The tracking error monotonically converges as

$$\|\tilde{B}_i\tilde{r} - y_{1,1}(k+1)\| \leq \big(I + \underline{\sigma}(\tilde{G}_i\tilde{G}_i^* Q)\big)^{-1} \|\tilde{B}_i\tilde{r} - y_{1,1}(k)\|$$

with $\lim_{k\to\infty} y_{1,1}(k) = \tilde{B}_i\tilde{r}$. The control action converges to the ideal input $\bar{w}_2^{P_i} := (-(\tilde{G}_i^{-1}\tilde{B}_i - \tilde{H}_i)\tilde{r}, 0, -\tilde{B}_i\tilde{r}, \tilde{r})^\top$.

Proof: Involves extensive manipulations to give $I + \tilde{Z}_{i,i}\tilde{L}_i = I + \tilde{G}_i\tilde{G}_i^* Q$ where $\tilde{Z}_{i,j} = \big(I - \tilde{G}_i\tilde{N}_j\big)^{-1}\tilde{G}_i$. ∎

The next result establishes stability bounds with disturbance and model mismatch. We consider a plant P_i (comprising G_i, H_i) that is switched into closed loop with an arbitrary controller C_j (comprising N_j, L_j, B_j).

Proposition 3: 1) (Linear growth of $[P_i, C_j]$): Let $P = P_i$ and $C = C_j$ be given by (11) with the signal connections of Fig. 2. Let $l_1, l_2, l_3, l_4 \in \mathbb{N}$, $l_1 < l_2 \leq l_3 < l_4$ and $I_1 = [l_1, l_2)$, $I_2 = [l_2, l_3)$, $I_3 = [l_3, l_4)$. Then the control signal w_2 is bounded with respect to the ideal solution for plant P_i of $\bar{w}_2^{P_i} = \big(-(\tilde{G}_i^{-1}\tilde{B}_j - \tilde{H}_i)\tilde{r}, 0, -\tilde{B}_j\tilde{r}, \tilde{r}\big)^\top$ by

$$\begin{aligned} &\|w_2|_{I_3}\|_{\bar{w}_2^{P_i}} \leq \\ &\underbrace{\left\| \begin{bmatrix} \|I + \tilde{L}_j\tilde{Z}_{i,j}\|^{|I_2|+1} \\ \vdots \\ \|I + \tilde{L}_j\tilde{Z}_{i,j}\|^{|I_2|+|I_3|} \end{bmatrix} \right\| \|I - \tilde{N}_j\tilde{G}_i\| \|(I - \tilde{N}_j\tilde{G}_i)^{-1}\| \|w_2|_{I_1}\|_{\bar{w}_2^{P_i}}}_{\alpha(P_i, C_j, |I_2|, |I_3|)} \\ &+ \underbrace{\left\| \begin{bmatrix} (\bar{\Lambda}_{i,j}^{|I_2|+1} + \bar{X}_{i,j}^{|I_2|+1}) & \bar{X}_{i,j}^{|I_2|} & \cdots \bar{X}_{i,j}^{1}\bar{\Gamma}_{i,j} \\ \vdots & \vdots & \vdots \ \vdots \ \ddots \ \ddots \\ (\bar{\Lambda}_{i,j}^{|I_2|+|I_3|} + \bar{X}_{i,j}^{|I_2|+|I_3|}) & \bar{X}_{i,j}^{|I_2|+|I_3|-1} & \cdots \cdots \cdots \bar{X}_{i,j}^{1}\bar{\Gamma}_{i,j} \end{bmatrix} \right\|}_{\beta(P_i, C_j, |I_2|, |I_3|)} \\ &\cdot \|w_0|_{I_1 \cup I_2 \cup I_3}\| \end{aligned} \tag{13}$$

where $\bar{\Lambda}_{i,j}^q = -(I - \tilde{N}_j\tilde{G}_i)^{-1}(I + \tilde{L}_j Z_{i,j})^q \tilde{N}_j \bar{A}_{i,j}$, $\bar{X}_{i,j}^q = (I - \tilde{N}_j\tilde{G}_i)^{-1}(I + \tilde{L}_j Z_{i,j})^{q-1}\tilde{L}_j(I - \tilde{G}_i\tilde{N}_j)^{-1}\bar{A}_{i,j}$, $\bar{\Gamma}_{i,j} = (I - \tilde{N}_j\tilde{G}_i)^{-1}\tilde{N}_j\bar{A}_{i,j}$. Here $\bar{A}_{i,j} = (-\tilde{G}_i, -\tilde{G}_i\tilde{H}_i, I, \tilde{B}_j)$.
2) (Stability of $[P_i, C_i]$): Let $x \in \mathbb{N}$, then

$$\alpha(P_i, C_i, a, x) \to 0 \ \text{ as } \ a \to \infty \tag{14}$$

and α is monotonic in a.

Proof: Follows after extensive manipulations and the identity $\|\|x\|, \|y\|\| = \|(x, y)\|$, $x, y \in l_2$. ∎

Stablising controller design procedure

$$\Psi : \mathcal{P} \to \mathcal{C} \tag{15}$$

Estimator

$$\begin{aligned} X : \mathcal{W}_e &\to map(\mathbb{N}, map(\mathcal{P}, \mathbb{R}^+)) \\ : w_2 &\mapsto [k \to (i \mapsto r_i[k])] \end{aligned} \tag{16}$$

Minimising operator

$$\begin{aligned} \hat{M} : (map(\mathbb{N}, map(\mathcal{P}, \mathbb{R}^+))) &\to map(\mathbb{N}, \mathcal{P}^*) \\ : \big[k \mapsto (i \mapsto r_i[k])\big] &\mapsto \big[k \mapsto q_f(k)\big] \end{aligned} \tag{17}$$

$$q_f(k) := \underset{i \in G}{\operatorname{argmin}}\, r_i[k], \ \forall k \in \mathbb{N} \tag{18}$$

Delay transition operator

$$\begin{aligned} D : map(\mathbb{N}, \mathcal{P}^*) &\to map(\mathbb{N}, \mathcal{P}^*) \\ : [k \mapsto q_f(k)] &\mapsto [k \mapsto q(k)] \end{aligned} \tag{19}$$

$$q(k) := \begin{cases} q_f(k) & \text{if} \quad k - k_s(k) \geq \Delta(q(k_s(k))) \\ q(k_s(k)) & \text{else} \end{cases} \tag{20}$$

$$\Delta : \mathcal{P} \to \mathbb{N} \tag{21}$$

$$k_s(k) := \max\{i \in \mathbb{N} \mid 0 \leq i \leq k, \ q(i) \neq q(i-1)\} \tag{22}$$

Overall switching operator

$$S : \mathcal{W}_e \to map(\mathbb{N}, \mathcal{P}^*) : w_2 \mapsto q \tag{23}$$

$$S = \hat{D}\hat{M}(X, \mathcal{G}) \tag{24}$$

Controller

$$C : \mathcal{Y}_e \to \mathcal{U}_e : y_2 \mapsto u_2 \tag{25}$$

$$u_2(k) = \Psi(q(k))(y_2 - \mathcal{T}_{k_s(k)-1} y_2)(k) \tag{26}$$

TABLE I
EQUATIONS SPECIFYING THE EMMILC ALGORITHM.

IV. EMMILC TRACKING STRUCTURE

EMMILC was introduced in [8] and comprises the switching algorithm illustrated in Fig. 3. The corresponding structural requirements are shown in Table I. The control design procedure Ψ assigns a stabilising controller $C_i \in \mathcal{C}$ to each plant $P_i \in \mathcal{P}$, such that $[P_i, C_i]$ is gain stable. The powerset of $\mathcal{P}$ is denoted $\mathcal{P}^*$ and $\mathcal{G} \subset \mathcal{P}$ is a constant set of candidate plant models thought to represent the true plant. For each $P_i \in \mathcal{G}$ we implement an estimator X which uses observations w_2 to generate a residual $r_i[k]$ at sample k. These are fed to the minimization operator $\hat{M}$, which returns the index, q_f, of the plant with minimal residual. The purpose of operator D is to delay the free switching signal q_f long enough to prevent instability effects caused by rapid switching, and so ensure overall convergence of the closed-loop signals. For this purpose we associate with every plant a minimum delay $\Delta(i)$ which must elapse before another is permitted. The signal q then determines the atomic controller choice $\Psi(q(k))$ corresponding to the selected plant. Together these components comprise the switching operator S shown in Fig. 3, where P_* denotes the true plant.

A. Estimation Problem

Estimator X is selected as the biased infinite horizon operator, defined for each P_i as

$$r_i[k] = X(w_2)(k)(P_i) = \inf\{\|v\|, v \in \mathcal{N}_i^{[0,k]}(w_2)\} \tag{27}$$

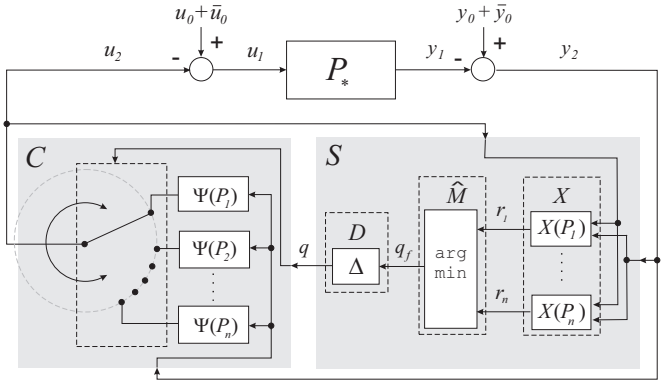

Fig. 3. EMMILC structure: switch S outputs switching signal q which determines the controller choice $C_{\Psi(q(k))}$. Here q is generated via delay operator D from free switching signal q_f, which in turn is generated from minimization operator $\hat{M}$ acting on residuals $r_i[k]$ from estimator X.

where the set of weakly consistent disturbance signals for plant P_i and observation $w_2 = (u_2, y_2)^\top$ with bias $\bar{w}_0 = (\bar{u}_0, \bar{y}_0)^\top$ over trials $k = a, \cdots, b$ is

$$\mathcal{N}_{i,\bar{w}_0}^{[a,b]}(w_2) := \Big\{ v \in \mathcal{W}|_{[a,b]} \mid \exists (u_0, y_0)^\top \in \mathcal{W}_e \text{ s.t.} \\ \mathcal{R}_{b-a,b} P_i\big(u_0 + \bar{u}_0 - u_2\big) = \mathcal{R}_{b-a,b}\big(y_0 + \bar{y}_0 - y_2\big), \\ v = (\mathcal{R}_{b-a,b} u_0, \mathcal{R}_{b-a,b} y_0) \Big\} \quad (28)$$

where the restriction operator $\mathcal{R}_{\sigma,t} v := (v(t-\sigma), \cdots, v(t))$. This is computed as follows.

Theorem 1: Residual (27) is given by

$$r_i[k] = \sum_{b=0}^{k} \left\| \left(\begin{pmatrix} I & 0 \\ 0 & I \\ \tilde{G}_i & \tilde{G}_i \tilde{H}_i \\ 0 & 0 \end{pmatrix} \begin{pmatrix} I & 0 \\ 0 & I \\ \tilde{G}_i & \tilde{G}_i \tilde{H}_i \\ 0 & 0 \end{pmatrix}^\dagger - \begin{pmatrix} I\,0\,0\,0 \\ 0\,I\,0\,0 \\ 0\,0\,I\,0 \\ 0\,0\,0\,I \end{pmatrix} \right) \\ \cdot \begin{pmatrix} 0 \\ 0 \\ \tilde{G}_i\big(u_{2,1}(b) - \tilde{H}_i \tilde{r}\big) - y_{2,1}(b) \\ \tilde{r} - y_{2,2}(b) \end{pmatrix} \right\| \quad (29)$$

Proof: Since the plant dynamics along each pass are independent of the previous pass, we can write

$$\mathcal{N}_{i,\bar{w}_0}^{[0,k]}(w_2) = \mathcal{N}_{i,\bar{w}_0}^{[0,0]}(w_2) \times \mathcal{N}_{i,\bar{w}_0}^{[1,1]}(w_2) \times \cdots \times \mathcal{N}_{i,\bar{w}_0}^{[k,k]}(w_2).$$

This means residual (27) can be obtained recursively as

$$r_i[k] = \sum_{b=0}^{k} i_i[b] \quad \text{with} \quad i_i[b] := \inf\{\|v\| \in \mathcal{N}_i^{[b,b]}(w_2)\}$$

Within (28), the restriction becomes $\mathcal{R}_{0,b} v = v(b)$, and since P_i is a static mapping

$$\mathcal{R}_{0,b} P_i\big(u_0 + \bar{u}_0 - u_2\big) = \tilde{P}_i\big(u_0(b) + \bar{u}_0(b) - u_2(b)\big)$$

so that

$$\mathcal{N}_i^{[b,b]}(w_2) := \Big\{ v \in \mathcal{W}|_{[b,b]} \mid \exists (u_0, y_0)^\top \in \mathcal{W}_e \text{ s.t.} \\ \tilde{P}_i\big(u_0(b) + \bar{u}_0(b) - u_2(b)\big) = y_0(b) + \bar{y}_0(b) - y_2(b), \\ v = (u_0(b), y_0(b)) \Big\}. \quad (30)$$

Since

$$y_0(b) = \tilde{P}_i\big(u_0(b) + \bar{u}_0(b) - u_2(b)\big) - \bar{y}_0(b) + y_2(b) \quad (31)$$

we obtain $i_{i,\bar{w}_0}[b] =$

$$\inf_{\substack{u_0(b) \in \\ l_2^m[0,T]}} \left\{ \left\| \begin{pmatrix} u_0(b) \\ \tilde{P}_i\big(u_0(b) + \bar{u}_0(b) - u_2(b)\big) - \bar{y}_0(b) + y_2(b) \end{pmatrix} \right\| \right\}$$

whose solution yields (29). ∎

Computational load of (29) is high and grows with increasing k. However, with suitable choice of weighting, the residual can be computed by a Kalman filter designed for the along-the-trial system $\tilde{G}_i$, and driven by input $\tilde{H}_i \tilde{r} - u_{2,1}(b)$.

Theorem 2: Residual (29) can be efficiently computed by

$$r_i[k] = \sum_{b=0}^{k} \left[\sum_{t=0}^{T} \|\tilde{y}_{2,1}(b,t) + C_G \hat{x}(b,t)\|^2_{[C_G \Sigma(t) C_G^\top + I]^{-1}} \right]^{\frac{1}{2}}. \quad (32)$$

where the Kalman filter is implemented on trial b by

$$\begin{aligned} \hat{x}(b, t+1/2) &= \hat{x}(t) - \Sigma(t) C_G^\top [C_G \Sigma(t) C_G^\top + I]^{-1} \\ &\quad \cdot [\tilde{y}_{2,1}(b,t) + C_G \hat{x}(t)] \\ \Sigma(t+1/2) &= \Sigma(t) - \Sigma(t) C_G^\top [C_G \Sigma(t) C_G^\top + I]^{-1} C_G \Sigma(t) \\ \hat{x}(b, t+1) &= A_G \hat{x}(t+1/2) + B_G\big((\tilde{H}_i \tilde{r})(t) - \tilde{u}_{2,1}(b,t)\big) \\ \Sigma(t+1) &= A_G \Sigma(t+1/2) A_G^\top + B_G B_G^\top \end{aligned} \quad (33)$$

with $\hat{x}(b,0) = 0$, $\Sigma(0) = 0$.

Proof: Follows from the deterministic interpretation of the Kalman Filter, see e.g. [21]. ∎

V. NOMINAL STABILITY AND GAIN BOUNDS

The gain bounds that follow depend on the size and geometry of a 'cover' of the plant uncertainty set U, rather than on the plant uncertainty set itself. This enables the bounds to avoid scaling with the number of candidate models, unlike most multiple model frameworks. The notion of the cover is as follows. Let $A \subset \mathcal{P}$ be a plant set and let $\nu := map(\mathcal{P}, \mathbb{R}^+)$ be given. Now define for $P \in \mathcal{P}$

$$B_\delta(P, \nu(\hat{p})) := \{P\} \cup \big\{ P_1 \in \mathcal{P} \mid \delta(P, P_1) < \nu(P) \big\} \cap U,$$

to be the set of plants that reside within a neighbourhood of radius $\nu(P)$, as measured by gap δ, around P. For an appropriate choice of (A, ν), the union of the corresponding neighbourhoods in U then leads to a cover for U, so that

Definition 1: (A, ν) is a cover for uncertainty set U if $U \subset \big\{ \cup_{P \in A} B_\delta(P, \nu(P)) \big\}$.

We next give gain bounds for the interconnection of the controller with 'true' plant P_*, with components G_*, H_*.

Theorem 3: Let control design Ψ be such that given P_i, and $C_i = \Psi(P_i)$ is defined by (11). Let $P_* \in U$ where U is an LTI uncertainty set of appropriate dimensions we seek to control. Suppose (A, ν) is a finite cover for U. Let $\mathcal{G} \subset \mathcal{P}$ be a suitable sampling of U specifying the available candidate plant set. Suppose

$$\exists\, P \in \mathcal{G},\ \delta(P, P_*) < \varepsilon\ \chi_\nu(A, \nu) \quad (34)$$

for $\varepsilon > 0$. If

$$\pi(U, H, \nu, \varepsilon, P_*) > 0, \tag{35}$$

then the control scheme defined by (16)-(26) with estimator (32)-(33) and delay Δ satisfying $\sup_{P\in U} \alpha(P_i, \Psi(P_i), \Delta - 1, 1) < 0.5$ achieves the bound

$$\|\mathcal{T}_k w_2\|_{\bar{w}_2^{P_*}} \leq \hat{\gamma}(U, A, \nu, \varepsilon, P_*)\|w_0\| \tag{36}$$

where $\mathcal{T}_k$ is the truncation operator, the ideal control input for the true plant is $\bar{w}_2^{P_*}(k) = \big(-(\tilde{G}_{P_*}^{-1}\tilde{B}_{q(k)} - \tilde{H}_{P_*})\tilde{r}, 0, -\tilde{B}_{q(k)}\tilde{r}, \tilde{r}\big)^\top$ and χ_ν, π, $\hat{\gamma}$ are defined in Table II.

Proof: Generalises the EMMILC proof [8] to include multiple permissible reference trajectories for each candidate plant, resulting in a time-varying $\bar{w}_2^{P_*}$ that is explicitly extracted from the observed data via the estimator bank. ■

This theorem establishes that EMMILC can provide robust convergence to the ideal tracking solution for the true plant. This solution, $\tilde{B}_{q(k)}$, is selected by the estimator bank to correspond to the patient's voluntary intention. Theorem 3 provides transparent selection of G: (35) gives a maximum value of $\rho = \varepsilon\chi_\nu(A, \nu)$, which is used in (34) to specify a maximum distance between the models in G. This distance is measured by the gap metric in either lifted or unlifted plant space. Hence G is designed by constructing a covering of U by neighbourhoods of radius ρ with centre $P_i \in G$.

VI. Simulation Example

The control scheme is now applied to the upper limb stroke rehabilitation platform of [11], in which elbow extension is assisted via FES applied to the triceps. The task is a single 'point-to-point' movement of a single joint, hence $m = o = 1$, $p = 1$, $o_1 = 1$ with $\tilde{r} = 2$ rads. The maximum sample number T is fixed at 400 in all tests, with padding applied for attempts finishing earlier. The candidate plants P_i comprise:

- $\tilde{B}_i$: the minimum jerk solution for T_i samples, [5].
- $\tilde{K}_{\mathrm{ff},i}$, $\tilde{K}_{\mathrm{fb},i}$: proportional gain, k_i for simplicity.
- $\tilde{F}_i$: critically damped muscle dynamics $F_i(s) = \omega_i^2/(s^2 + 2\zeta_i\omega_i s + \omega_i^2)$, as shown to accurately capture muscle dynamics [6]. The sampling period is 0.01 s.

Together these yield G_i, H_i via (1), (2), and are therefore each candidate P_i is parametrised by the set $\{T_i, k_i, \omega_i, \zeta_i\}$.

We define the true plant P_* analogously, with $\zeta_* = 1$, $\omega_* = 5$, $k_* = 0.5$, $T_* = 320$ on trials 1 to 14, and then subsequently with $\zeta_* = 0.7$, $\omega_* = 8$, $k_* = 0.3$, $T_* = 200$. This represents a rapid onset of fatigue, associated with faster dynamics and weaker voluntary effort. The candidate plant set $\mathcal{G}$ is designed via Theorem 3 and comprises all combinations of the following elements:

$$\zeta_i = \{0.4, 0.7, 1.0, 1.3, 1.6\}, \qquad \omega_i = \{2, 5, 8, 11\},$$
$$k_i = \{1, 2, 3, 4, 5, 6, 7, 8\}, \qquad T_i = \{220, 260, 300, 340, 380\}$$

The true plant response is shown in Fig. 4 and illustrates the level of voluntary input.

The control design $C_i = \Psi(P_i)$ is defined by (11) with $Q = 10$. The results are shown in Fig. 5 and Fig. 6. These confirm that the EMMILC framework is able to accurately assist voluntary effort while adapting to the plant dynamics, the level of voluntary effort, and the required task.

Controller bounds with nominal plant

$$\alpha_{OP}(U) = 4 \sup_{P_1\in U} \alpha^2(P_1, \Psi(P_1), \Delta(P_1) - \sigma, \sigma)$$
$$\beta_{OP}(U) = 4 \sup_{\substack{\Delta(P_1)\leq x\leq 2\Delta(\hat{p}_1)\\ P_1\in U}} \beta^2(P_1, \Psi(P_1), x - \sigma, \sigma)$$
$$\alpha_{OS}(U) = 4 \sup_{\substack{\Delta(P_1)\leq x\leq 2\Delta(\hat{p}_1)\\ P_1\in U}} \alpha^2(P_1, \Psi(P_1), 0, x - \sigma)$$
$$\beta_{OS}(U) = 4 \sup_{\substack{\Delta(P_1)\leq x\leq 2\Delta(\hat{p}_1)\\ P_1\in U}} \beta^2(P_1, \Psi(P_1), 0, x - \sigma)$$

$$\gamma_3(U) = (1 + \alpha_{OS}^{1/2}(U))\left(\frac{\alpha_{OP}(U)}{1 - \alpha_{OP}(U)}\right)^{1/2} + \alpha_{OS}^{1/2}(U) \tag{37}$$

$$\gamma_4(U) = (1 + \alpha_{OS}^{1/2}(U))\left(\frac{\beta_{OP}(U)}{1 - \alpha_{OP}(U)}\right)^{1/2} + \beta_{OS}^{1/2}(U) \tag{38}$$

Controller bounds with real plant

$$\gamma_1(P, P_*) = 1 + \sup_{\Delta(P)\leq x\leq 2\Delta(P)} \alpha(P_*, \Psi(P), 0, x)$$
$$\gamma_2(P, P_*) = \sup_{\Delta(P)\leq x\leq 2\Delta(P)} \beta(P_*, \Psi(P), 0, x),$$
$$\bar{\gamma}_i(Q_1, Q_2) = \sup_{P_1\in Q_1}\sup_{P_2\in Q_2} \gamma_i(P_1, P_2),\ i = 1, 2$$

Gain bound

$$\hat{\gamma}(U, A, \nu, \varepsilon, P_*) = \left(\sum_{P\in A}\gamma_2(P, P_*) + \frac{\gamma_4(U)\eta(H, \nu, \varepsilon, P_*)}{\pi(U, H, \nu, \varepsilon, \hat{p}_*)}\right)\phi(U, A, \nu, \varepsilon, P_*) \tag{39}$$

where

$$\pi(U, A, \nu, \varepsilon, P_*) = 1 - 2^{1/2}\varepsilon\chi_\nu(A, v)(1 + \bar{\gamma}_1^2(A, U))\gamma_4(U)$$
$$\eta(A, \nu, \varepsilon, P_*) = 2^{1/2}(1 + \varepsilon\chi_\nu(A, \nu)\bar{\gamma}_2(A, P_*)(1 + \bar{\gamma}_1(A, P_*)))$$
$$\phi(U, A, \nu, \varepsilon, P_*) = \left(\frac{1 + \gamma_3(U)}{\pi(U, A, \nu, \varepsilon, P_*)}\right)^{|A|}\prod_{P\in A}\gamma_1(P, P_*)$$
$$\chi_\nu(H, \nu) = 2\sup_{P\in A}\nu(P) \text{ where } \nu : \mathcal{P} \to \mathbb{R}^+ \tag{40}$$

TABLE II

Functions specifying the EMMILC gain bound.

VII. Conclusion

A multiple model ILC framework has been developed which is capable of assisting human motor control. This is the first approach to combine ILC and models of human motor control, and is motivated by the need of stroke rehabilitation to precisely assist patient's voluntary completion of functional tasks. A key feature of the framework is its potential to remove the need for model identification and controller tuning. Future work will focus on applying the framework to stroke patients within clinical feasibility trials.

Acknowledgment

This work was supported by the Engineering and Physical Sciences Research Council (grant ref: EP/M026388/1) and Medical Research Council (grant ref: MR/N027841/1).

References

[1] P. M. Aubin, M. S. Cowley, and W. R. Ledoux, "Gait simulation via a 6-DOF parallel robot with iterative learning control," *IEEE Trans Biomedical Engineering*, vol. 55, pp. 1237–1240, 2008.

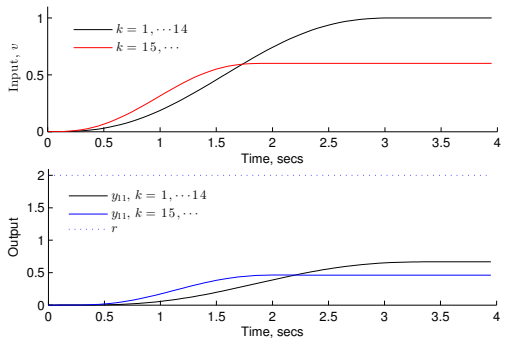

Fig. 4. Voluntary signals G_*r, G_*H_*r of true plant P_* (i.e. no FES).

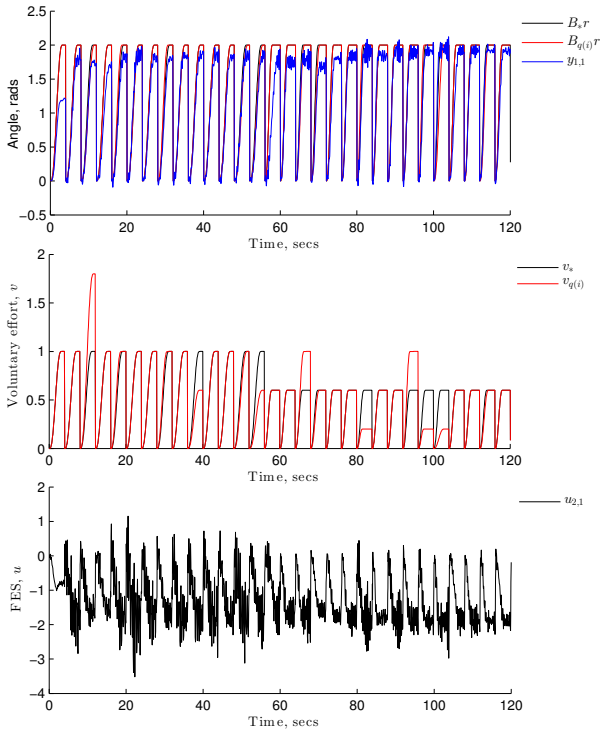

Fig. 5. Tracking results (top), estimated voluntary effort (middle) and applied FES (bottom) for $Q = 10$.

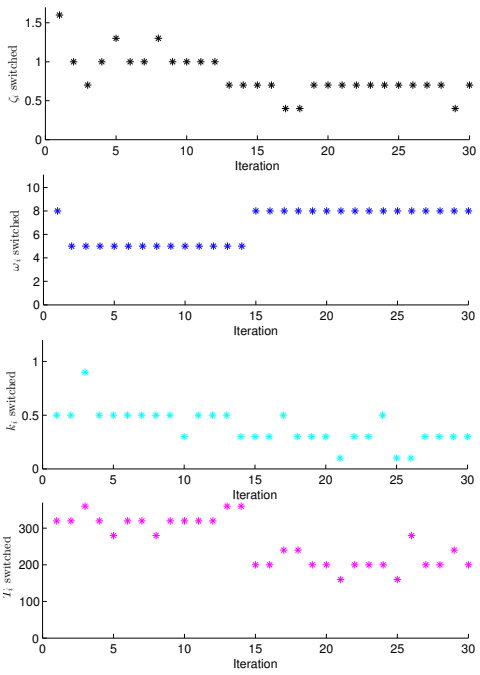

Fig. 6. Switching signals for parameters with candidate plants for $Q = 10$.

[2] J. Bae and M. Tomizuka, "A gait rehabilitation strategy inspired by an iterative learning algorithm," *Mech*, vol. 22, no. 2, pp. 213–221, 2012.

[3] D. Buchstaller and M. French, "Robust stability and performance for multiple model adaptive control: Part i - the framework," *IEEE Transactions on Automatic Control*, vol. 61, no. 3, pp. 677–692, 2016.

[4] ——, "Robust stability and performance for multiple model adaptive control: Part ii - gain bounds," *IEEE Transactions on Automatic Control*, vol. 61, no. 3, pp. 693–708, 2016.

[5] T. Flash and N. Hogan, "The coordination of arm movements: An experimentally confirmed mathematical model," *Journal of Neuroscience*, vol. 5, pp. 1688–1703, 1985.

[6] C. T. Freeman, *Control System Design for Electrical Stimulation in Upper Limb Rehabilitation*, ser. Springer International Publishing. Springer International Publishing, 2016.

[7] ——, "Robust ILC design for electrical stimulation in upper limb rehabilitation," *Automatica*, vol. 81, pp. 270–278, 2017.

[8] C. T. Freeman and M. French, "Estimation based multiple model iterative learning control," in *54th IEEE Conference on Decision and Control*, 2015, pp. 6075–6080.

[9] T. T. Georgiou and M. C. Smith, "Optimal robustness in the gap metric," *IEEE Trans Automatic Control*, vol. 35, no. 6, pp. 673–686, sep 1990.

[10] C. M. Harris and D. M. Wolpert, "Signal-dependent noise determines motor planning," *Nature*, vol. 20, no. 394(6695), pp. 780–784, 1998.

[11] A. M. Hughes, C. T. Freeman, J. H. Burridge, P. H. Chappell, P. Lewin, and E. Rogers, "Feasibility of iterative learning control mediated by functional electrical stimulation for reaching after stroke," *J Neurorehab Neural Repair*, vol. 23, no. 6, pp. 559–568, 2009.

[12] C. Klauer and T. Schauer, "Adaptive control of a neuroprosthesis for stroke patients amplifying weak residual shoulder-muscle activity," in *20th IFAC World Congress. Toulouse, France*, 2017, pp. 9122–9127.

[13] E. Langzam, Y. Nemirovsky, E. Isakov, and J. Mizrahi, "Partition between volitional and induced forces in electrically augmented dynamic isometric muscle contractions," *IEEE Transactions on Neual Systems and Rehabilitation Engineering*, vol. 13, no. 3, 2006.

[14] K. L. Meadmore, T. Exell, E. Hallewell, A.-M. Hughes, C. T. Freeman, M. Kutlu, V. Benson, E. Rogers, and J. H. Burridge, "The application of precisely controlled functional electrical stimulation to the shoulder, elbow and wrist for upper limb stroke rehabilitation: A feasibility study," *Journal of NeuroEngineering and Rehabilitation*, vol. 11, p. 105, 2014.

[15] K. L. Meadmore, A.-M. Hughes, C. T. Freeman, Z. Cai, D. Tong, J. H. Burridge, and E. Rogers, "Functional electrical stimulation mediated by iterative learning control and 3*d* robotics reduces motor impairment in chronic stroke," *Journal of Neuroengineering and Rehabilitation*, vol. 32, no. 9, pp. 1–11, 2012.

[16] H. Nahrstaedt, T. Schauer, S. Hesse, and J. Raisch, "Iterative learning control of a gait neuroprosthesis," *Automatisierungs*, vol. 56, no. 9, pp. 494–501, 2008.

[17] K. Ohta, M. M. Svinin, Z. Luo, S. Hosoe, and R. Laboissiere, "Optimal trajectory formation of constrained human arm reaching movements," *Biological Cybernetics*, vol. 91, no. 1, pp. 23–36, 2004.

[18] D. H. Owens, C. T. Freeman, and T. V. Dinh, "Norm-optimal iterative learning control with intermediate point weighting: Theory, algorithms, and experimental evaluation," *IEEE Transactions on Control System Technology*, vol. 21, no. 3, pp. 999–1007, 2012.

[19] T. Seel, T. Schauer, and J. Raisch, "Iterative learning control for variable pass length systems," in *IFAC World Congress*, 2011, pp. 4880–4885.

[20] Y. Uno, M. Kawato, and R. Suzuki, "Formation and control of optimal trajectory in human multijoint arm movement." *Biological Cybernetics*, vol. 61, no. 2, pp. 89–101, 1989.

[21] J. C. Willems, "Deterministic least squares filtering," *Journal of Econometrics*, no. 118, pp. 341–370, 2004.